Research Article | Vol. 29, No. 25 / 6 Dec 2021 / Optics Express 41766
Optics EXPRESS

Experimental quantification of the robustness of adiabatic rapid passage for quantum state inversion in semiconductor quantum dots

A. RAMACHANDRAN,[1] J. FRASER-LEACH,[1] S. O'NEAL,[2,3] D. G. DEPPE,[2,4] AND K. C. HALL[1,*]

[1]*Department of Physics and Atmospheric Science, Dalhousie University, Halifax, Nova Scotia B3H 4R2, Canada*
[2]*The College of Optics and Photonics, University of Central Florida, Orlando, Florida 32816-2700, USA*
[3]*Present Address: Imec, Kissimmee, Florida, 34744, USA*
[4]*Present Address: SdPhotonics, Richardson, Texas 75081, USA*
[*]*Kimberley.Hall@dal.ca*

Abstract: Adiabatic rapid passage (ARP) is demonstrated in a single In(Ga)As quantum dot (QD) over a wide range of laser tuning relative to the exciton transition energy to assess the level of robustness of this quantum state inversion gate for practical QD systems. Our experiments indicate a drop in exciton inversion by only 5% for a detuning of 9.3 meV, indicating accessible detunings that span the typical inhomogeneous broadening of self-assembled QD ensembles. Our findings indicate that ARP is an ideal control protocol for synchronous triggering of quantum light sources for applications in photonic quantum technology.

1. Introduction

Efficient, on-demand sources of single and entangled photons are needed for applications such as linear optical quantum computing [1] and distributed quantum networks [2], which utilize the quantum state of a photon (a so-called flying qubit) for transferring and/or manipulating information. Semiconductor QDs are promising for these applications due to their strong optical transitions [3–5], high optical coherence [2], large internal quantum efficiency enabling a high photon generation rate [2], and the ease with which they may be integrated into photonic structures for efficient photon extraction [6–8]. These favorable properties have led to the demonstration of single photon sources with high photon purity and indistinguishability [9–18] and entangled photon sources with near unity entanglement fidelity [19–24]. For such sources, optimum performance is achieved using resonant excitation of the ground state (GS) or the first excited state (ES) transition in the QD, which avoids the deleterious effects of multiple carrier capture events and fluctuating charges tied to nonresonant pumping schemes [7,8].

The development of scalable networks requires the integration of multiple, synchronous quantum light sources that can be triggered in parallel using a single pulsed laser source [2,13,15,17,18,25,26]. The inhomogeneity in the QD optical transition energy due to QD size variations typical of a QD ensemble represents a barrier to parallel excitation of multiple QD sources since the strictly resonant tuning condition required for conventional excitation using a Rabi rotation [4,5,27–30] can only be satisfied for a small fraction of the QDs. An ideal quantum state preparation scheme for triggering photon emission would be insensitive to variations in the QD optical transition energy while simultaneously enabling resonant driving of the excitonic system. ARP uses frequency-swept laser pulses to invert the state of the exciton by adiabatically transferring the system through an anti-crossing between the dressed states of the QD in the presence of the light field [31–33]. ARP provides a more robust approach to quantum state inversion than a Rabi rotation because, provided the system is initially in the ground state, the

#435109 https://doi.org/10.1364/OE.435109
Journal © 2021 Received 28 Jun 2021; revised 20 Aug 2021; accepted 2 Sep 2021; published 1 Dec 2021
Corrected: 13 December 2021

Optics EXPRESS

dressed state is uniquely identified with the exciton at the end of the laser pulse. ARP has been demonstrated in single QDs for inverting excitons [34–37] and biexcitons [38], for realizing a triggered QD single-photon source [39] and for demonstrating dynamic decoupling in the strong driving regime [40,41]. In all cases, the chirped laser pulse used to carry out ARP was resonant with the excitonic transition in the QD. Determination of the level of robustness of ARP to variations in the QD transition energy would facilitate the extension of this technique to triggering multiple QD emitters.

In experiments on a single In(Ga)As/GaAs QD, we show here that high-fidelity quantum state inversion is possible over a large range of laser detuning from the QD transition energy using ARP implemented by shaped, broad bandwidth laser pulses. In contrast to the case of Rabi rotations, for which the laser detuning dependence of the exciton inversion follows the spectrum of the laser source and is highly sensitive to changes in pulse area, our findings indicate that ARP provides high fidelity inversion over a wide bandwidth of photon energies ~20 meV, similar to the inhomogeneous linewidth of typical self-assembled QD ensembles [42–44]. For comparison, in recently-developed approaches to quasi-resonant driving of QDs based on phonon-assisted excitation [15,45,46], the detuning is limited to the 1-2 meV width of the phonon spectral density [47,48]. For applications of single-photon sources requiring photon indistinguishability [7], our experiments remove the simultaneous need for different QD emitters to exhibit equal GS emission energies and energy separations between the GS and ES optical transitions [42–44] since ARP enables the ES in inequivalent emitters to be driven far from resonance. Our simulations of the quantum state dynamics incorporating coupling to LA-phonons indicate that suppression of phonon-induced transitions between the dressed states of the QD, which unlike other control schemes is possible for ARP using a positively chirped control pulse [36], is essential to maintain the level of robustness we report here.

2. Adiabatic rapid passage

ARP utilizes a frequency-swept laser pulse, given by $E(t) = \frac{1}{2}E_p(t)\exp[-i(\omega_l t + \alpha t^2)]$, where $E_p(t)$ is the pulse envelope, ω_l is the center frequency of the laser pulse, and α is the temporal chirp [31–33]. The eigenstates of the QD in the presence of the laser field are the dressed states ($|\Psi_\pm\rangle$), each of which corresponds to a dynamic admixture of the bare QD states $|0\rangle$ and $|1\rangle$, where $|0\rangle$ ($|1\rangle$) represents the absence (presence) of a single exciton in the QD. The dressed state energies are shown in Fig. 1(a) for the case of resonant driving of the exciton transition in the QD. The energy splitting between the dressed states is given by $\sqrt{\Omega(t)^2 + \Delta(t)^2}$, where $\Omega(t) = \frac{\mu E_p(t)}{\hbar}$ is the Rabi frequency, μ is the dipole moment of the optical transition, $\Delta(t) = \Delta_0 - 2\alpha t$ is the instantaneous value of the detuning of the laser from the exciton transition frequency (ω_x), and $\Delta_0 = \omega_x$-ω_l is the static detuning, where for our conditions 2αt spans ±95 meV during the pulse. Unlike a Rabi rotation, for ARP the presence of chirp leads to a nonzero dressed state splitting $E_+ - E_-$ for all times during the control pulse. For a sufficiently large splitting at the anticrossing, the transition rate between the dressed states is negligible and the control process is adiabatic. The dressed states each undergo an evolution between $|0\rangle$ and $|1\rangle$, represented by darkness of the $E_\pm$ curves in Fig. 1(a), resulting in inversion of the quantum state of the exciton. The sign of the pulse chirp and the initial conditions together determine which dressed state the system remains in during the control process. For instance, if the exciton is initially in state $|0\rangle$, a positive (negative) value of α leads to state evolution via the lower (higher) energy dressed state.

The robustness of ARP for quantum state inversion follows from the condition for adiabatic evolution, given by $|\Delta\frac{d\Omega}{dt} - \Omega\frac{d\Delta}{dt}| \ll [\Omega^2 + \Delta^2]^{\frac{3}{2}}$ [33]. This condition, which is determined in part by the need to maintain a large enough dressed state splitting at the anticrossing, can be satisfied for a wide range of pulse parameters. For instance, once the adiabaticity condition is satisfied, increasing the pulse area (given by $\theta = \int_{-\infty}^{\infty}\frac{\mu E_p(t)}{\hbar}dt$) does not reduce the fidelity of

Optics EXPRESS

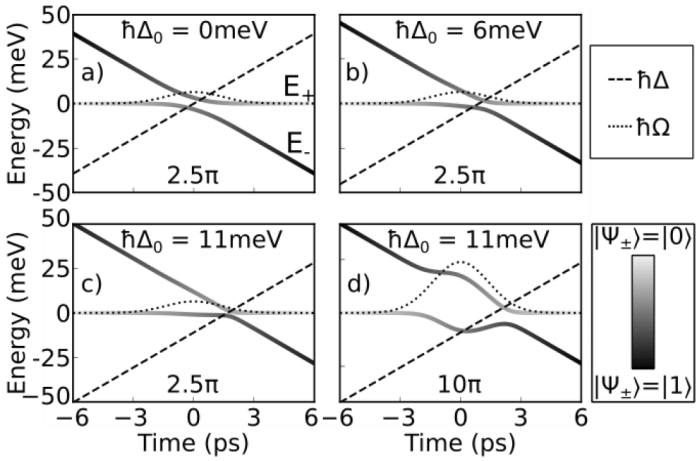

Fig. 1. Dressed state energies $E_{\pm}$ versus time for $\phi'' = 100{,}000$ fs^2 and $\theta = 2.5\pi$ for resonant excitation [(a)], and a red detuning of 6 meV [(b)], and 11 meV [(c)]. (d) Same as (c) but with $\theta = 10\pi$. The detuning ($\hbar\Delta$) and Rabi frequency ($\hbar\Omega$) are indicated by the dashed and dotted curves, respectively.

inversion. ARP is therefore insensitive to power fluctuations in the laser source, in contrast to Rabi rotations. The adiabatic condition may also be satisfied for a nonzero static detuning Δ_0. Our objective in this work is to explore the limits of this robustness experimentally for solid state emitters based on semiconductor QDs.

3. Quantum control experiments on single QDs

Quantum control experiments were carried out on a single InGaAs/GaAs QD with a GS transition at 1.259 μm. Further details regarding the QD sample are provided in Ref. [37]. A schematic diagram of the experimental apparatus is shown in Fig. 2(a). The sample is housed in a liquid-helium microscopy cryostat equipped with a nanopositioning stage. For all experiments reported here, the sample temperature was 10 K. The laser source is an optical parametric oscillator with a repetition rate of 76 MHz. For all experiments, the laser was circularly-polarized to suppress excitation of the biexciton transition in the QD. A 4f-pulse shaper equipped with multiphoton interference phase scan [49,50] results in a dispersion-compensated pulse duration (full-width at half maximum) at the sample position of $\tau_0 = 120$ fs. For ARP, the same 4f pulse shaper is used to impose spectral chirp (ϕ'', related to the temporal chirp α by $\alpha = 2\phi''/[\tau_0^4/(2\ln(2))^2 + (2\phi'')^2]$). The pulse shaping system contains a 128 pixel dual-mask spatial light modulator. The maximum phase gradient is $\frac{\pi}{10}$ radians per pixel with accessible spectral chirps up to $\phi'' \sim 500{,}000$ fs^2. Optical excitation was carried out on the ES transition in the QD at 1.162 μm determined using photoluminescence (PL) excitation measurements. A long working distance objective lens (Mitutoyo Plan APO NIR HR, NA = 0.87) is used for both focusing the excitation laser onto the sample and for collecting the emitted PL from the GS transition. The spot size of the OPO laser source on the sample is 1.9 μm. The PL from the GS transition was detected using a 0.75 m monochromator and a liquid nitrogen cooled InGaAs array detector with an overall energy resolution of 30 μeV. For additional details regarding the quantum control experiments, see Ref. [37,50] and Supplement 1.

Optics EXPRESS

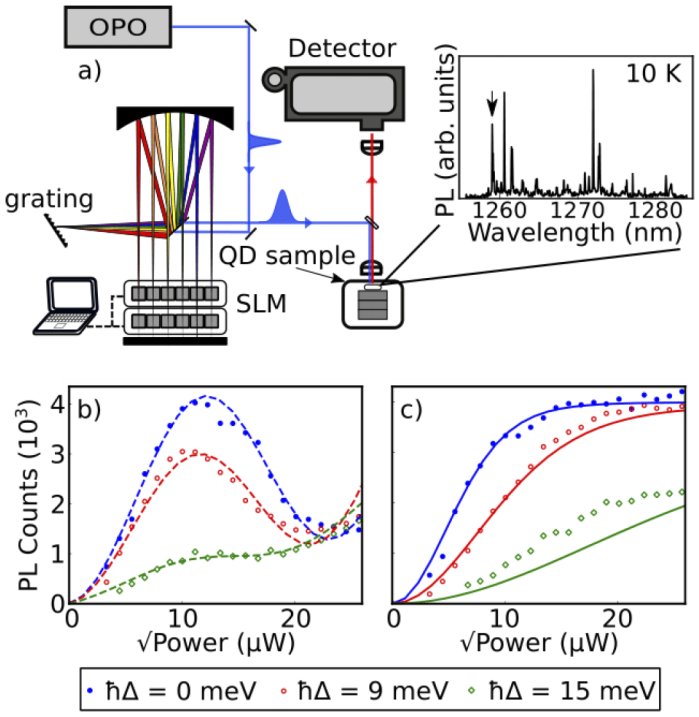

Fig. 2. (a) Schematic diagram of the quantum control apparatus. Inset: microPL from the QD sample. The QD used for the experiments is indicated by the arrow. (b) PL intensity versus pulse area for $\phi'' = 0$ for resonant excitation (blue filled circles) and a red detuning of 9 meV (red open circles) and 15 meV (green diamonds). (c) Same as (b) with a spectral chirp of $\phi'' = 0.3$ ps^2. The solid curves indicate the results of numerical simulations for $\phi'' = 0$ [(b)] and $\phi'' = 0.3$ ps^2 [(c)] including electron-phonon coupling (see Supplement 1). A linear background is included in the simulations for $\phi'' = 0$ and reflects QD pumping via two-photon absorption or other nonlinear excitation channel enhanced by the short duration of the unchirped pulse.

4. Results and discussion

The results of Rabi rotation experiments for laser detunings of $\hbar\Delta_0 = 0$ meV, 9 meV, and 15 meV are shown in Fig. 2(b). For resonant excitation, a damped Rabi oscillation is observed. The damping is induced by electron-LA phonon coupling [51–55]. As the laser is detuned from resonance, the amplitude of the Rabi oscillations drops rapidly, resulting in poor state inversion. For resonant driving using a Rabi rotation, the system is in an equal superposition of the two dressed states during the control pulse and the relative amplitudes of the bare QD states oscillate versus time. Only when the pulse area is an odd-multiple of π is the final state of the system $|1\rangle$. If the laser is detuned from the transition, the superposition of the dressed states is characterized by unequal amplitudes and the exciton occupation never reaches unity.

The results of ARP experiments for the same values of $\hbar\Delta_0$ as in Fig. 2(b) are shown in Fig. 2(c). For these experiments, the laser control pulse was positively-chirped to suppress the effect of LA-phonon coupling [36,38,41], as discussed further below. The results in Fig. 2(c) indicate that exciton inversion still occurs for ARP with a detuned pulse provided a sufficiently large pulse area is used. Experimental results corresponding to a full range of laser tuning are shown for a Rabi rotation in Fig. 3(a) and for ARP in Fig. 3(b). The maximum exciton inversion occurs for a narrow range of detunings and pulse areas for control using a Rabi rotation. In

Optics EXPRESS

contrast, for ARP the inversion is insensitive to changes in pulse area once θ is large enough to enter the adiabatic regime. This threshold occurs at a larger pulse area as Δ_0 is increased. As a result, the bandwidth of detunings for which maximum inversion occurs increases with increasing pulse area. For a pulse area of 2.5π, the exciton occupation drops by 5% when the laser is detuned by 9.3 meV. The results of calculations of the quantum state dynamics [56,57] are shown in Fig. 3(c) and Fig. 3(d), showing good agreement with the experimental results.

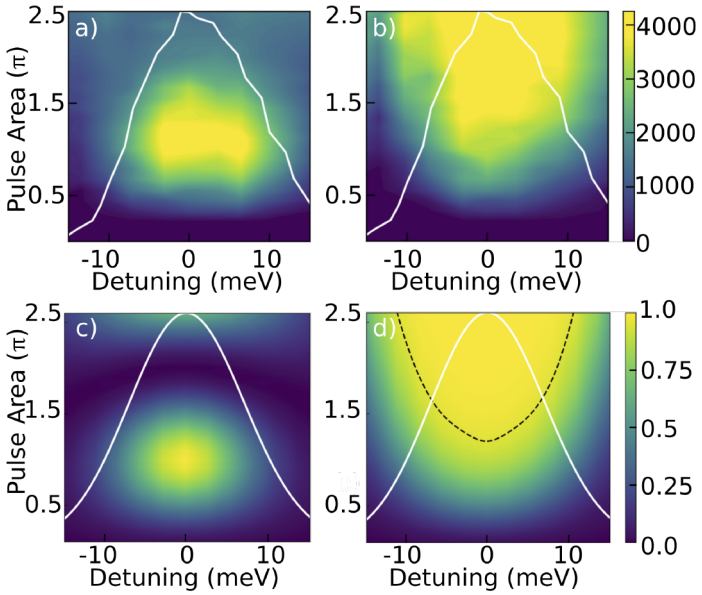

Fig. 3. (a)/(b) PL intensity versus detuning and pulse area for $\phi'' = 0$ [(a)] and $\phi'' = 0.3$ ps^2 [(b)]. The white curves indicate the laser spectrum. (c)/(d) Calculated exciton occupation for $\phi'' = 0$ [(c)] and $\phi'' = 0.3$ ps^2 [(d)]. The black dashed curve in (d) indicates the 0.95 contour line in the exciton occupation, representing a nearly-constant value of the dressed state splitting at the anticrossing of (1.9±0.05) meV.

The larger threshold pulse area required for adiabatic state transfer when the laser pulse is detuned from the excitonic transition may be understood by examining the dressed state energies ($E_\pm$) for resonant and detuned laser pulses, which are shown in Fig. 1(a)-(c). When Δ_0 is nonzero, the anticrossing shifts away from $t = 0$. If $|\Delta_0|$ is increased while keeping other pulse parameters fixed, the dressed state splitting at the anticrossing becomes smaller in magnitude. This decrease in the splitting results from the smaller value of Ω away from $t = 0$. Provided this smaller splitting still satisfies the adiabaticity condition, robust exciton inversion occurs, however for large enough Δ_0 diadiabatic transitions between the dressed states become significant and reduce the fidelity of quantum control. If Δ_0 is increased slightly beyond the adiabatic regime, high-fidelity inversion may be recovered by increasing the pulse area, which increases the value of Ω (and therefore the dressed state splitting) at the anticrossing. This is illustrated in Fig. 1(d), which shows the same detuning as in Fig. 1(c) but with 4 times larger pulse area. This interpretation is further supported by the dashed curve in Fig. 3(d), which shows the 0.95 contour line in the exciton occupation, representing a nearly-constant value of the dressed state splitting at the anticrossing of (1.9±0.05) meV. This accounts for the observed increase in the threshold pulse area for adiabatic passage when detuned pulses are used.

Figure 4 shows the calculated detuning bandwidth assuming a cutoff of 0.95 for the minimum required exciton inversion. These calculations were carried out using two different values of the laser pulse bandwidth (dictating the corresponding transform-limited pulse width τ_0) as a function

Optics EXPRESS

of the pulse area [Fig. 4(a)] and spectral chirp [Fig. 4(b)]. The detuning bandwidth increases monotonically for increasing pulse area. Much larger detunings are accessible for smaller τ_0, as expected due to the larger pulse bandwidth. For a given value of τ_0, the increase in the detuning bandwidth becomes slower at larger pulse areas because the dressed state splitting is relying on the tail of Ω at the anticrossing, as shown in Fig. 1(d). The detuning bandwidth also increases with increasing spectral chirp, as shown in Fig. 4(b), with the saturation value determined by τ_0. Since increases in ϕ'' also increase the control pulse duration, a compromise must be made to ensure that the control pulse used for quantum state inversion is as short as possible. For τ_0 = 120 fs, the detuning bandwidth exceeds 20 meV for ϕ'' = 100,000 fs^2, corresponding to a chirped control pulse duration of 2.3 ps. In contrast, using the same 0.95 cutoff value for the exciton occupation at inversion, the detuning bandwidth for Rabi rotations using τ_0 = 120 fs is less than 5 meV.

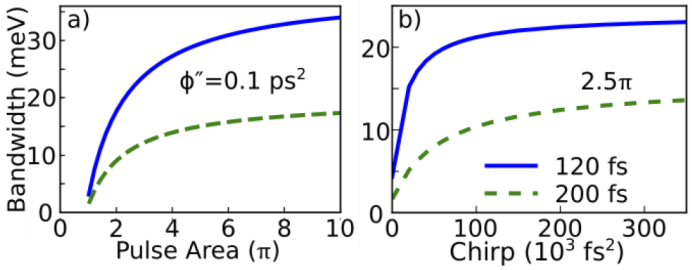

Fig. 4. Calculated detuning bandwidth assuming a minimum exciton occupation of 0.95 as a function of pulse area [(a)] and spectral chirp [(b)] for two different values of the pulse bandwidth. The curve labels indicate the corresponding transform-limited pulse duration.

The ability to achieve high-fidelity inversion over a wide range of laser detuning from the exciton transition in the QD would greatly facilitate the simultaneous pumping of multiple single photon sources using the same pulsed laser. The GS and ES optical transitions in typical self-assembled QD ensembles vary over a range of 10-30 meV [42–44,58,59]. In recent experimental demonstrations of two-photon interference involving remote QD sources [13,17,18,25], the QDs have either been excited nonresonantly via the wetting layer surrounding the QDs, which compromises the performance due to multiple carrier capture events [17,25], or individual QDs with near-identical size have been hand-picked out of the ensemble enabling the simultaneous resonant pumping of the ES transition within both QDs [13,17,18]. The latter approach is impractical for a scalable network due to the low yield of useful emitters. Our experiments show that ARP provides a robust method for realizing parallel quantum state inversion in distinct QD-based quantum emitters for either GS or ES pumping due to the broad bandwidth over which high fidelity inversion is achieved. The application of phonon-assisted excitation to the inversion of two QD single photon sources using the same laser source was recently demonstrated [15]. This scheme also exhibits robustness to detuning but over a much smaller spectral range to that reported here (a few meV) due to the limited bandwidth of the phonon spectral density [47,48].

Exciton-LA phonon coupling in the general case can lead to resonant transitions between the dressed states of the QD, limiting the fidelity of quantum control [47,48,51–53]. The rate of these transitions is governed by the phonon spectral density and the instantaneous value of the dressed state splitting. The ARP experiments in Fig. 2 and Fig. 3 utilized a positively-chirped laser pulse. Under these conditions, decoherence tied to phonon-induced transitions between the dressed states is suppressed at low temperatures because the system undergoes evolution through the anti-crossing via the lower-energy dressed state [36]. For a sufficiently large pulse area, this decoherence process may be suppressed at all temperatures and for both signs of pulse chirp. This is referred to as the decoupling regime and was recently demonstrated experimentally in

Optics EXPRESS

single InGaAs QDs [40,41]. Decoherence suppression occurs provided the minimum dressed state splitting exceeds the bandwidth of the LA phonon modes coupled to the exciton in the QDs, which is determined by the width of the phonon spectral density.

Here we explore the impact of detuning on the threshold pulse area required for decoherence suppression in numerical simulations of the quantum state dynamics incorporating LA-phonon coupling [36,57]. For these simulations, the in-plane diameter (height) of the QD was taken as 7.1 nm (5.7 nm), the exciton-LA phonon coupling strength was 0.0272 ps^2, and GS pumping was assumed. For further details regarding the numerical model see Ref [41] and Supplement 1 for supporting content. Figure 5(a) shows the calculated exciton occupation as a function of pulse area for $\hbar\Delta_0 = 11$ meV and Fig. 5(b) shows the corresponding results for resonant excitation. The

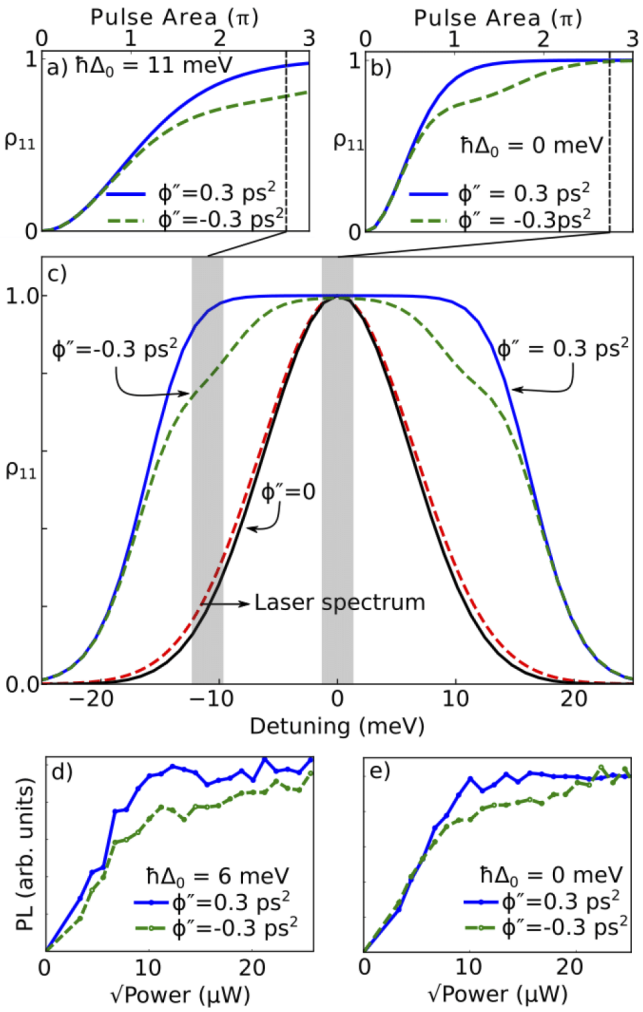

Fig. 5. (a) Calculated exciton occupation for positive (blue solid curve) and negative (green dashed curve) chirp with a magnitude of 0.3 ps^2 versus pulse area for a red detuning of $\hbar\Delta_0 = 11$ meV including exciton LA-phonon coupling. (b) Same as (a) for $\hbar\Delta_0 = 0$. (c) Calculated exciton occupation as a function of $\hbar\Delta_0$ at a pulse area of 2.75π. Red dashed curve: Laser Spectrum. Black solid curve: calculated exciton occupation for $\phi'' = 0$. (d) Measured chirp sign dependence of PL intensity for a detuning of $\hbar\Delta_0 = 6$ meV and chirp 0.3 ps^2. (e) Same as (d) for $\hbar\Delta_0 = 0$.

Optics EXPRESS

convergence of the calculated exciton occupation for positive and negative pulse chirp indicates suppression of LA-phonon induced decoherence [40,41]. For resonant excitation, the threshold pulse area for decoherence suppression is ~2.5π, but for the detuned pulse no convergence occurs over the range of pulse areas shown. These general trends are consistent with experimental results for detuned and resonant pulses in Fig. 5(d) and Fig. 5(e), respectively. Our calculations indicate that a pulse area exceeding 5π is required to suppress decoherence for a detuning of 11 meV. The higher threshold pulse area for decoherence suppression for the detuned pulse may be traced back to the smaller dressed state splitting at the anticrossing in Fig. 1(c), which must still exceed the bandwidth of the phonon spectral density to suppress decoherence. The calculated exciton inversion is shown in Fig. 5(c) for both signs of ϕ'' for a pulse area of 2.5π, indicating that ARP is less robust to detuning with negative pulse chirp. While the detuning bandwidth is larger for both signs of chirp for larger pulse areas, our results indicate that positive chirp should be used to obtain the maximum robustness at the smallest possible control pulse area.

5. Conclusion

In summary, we have demonstrated ARP on a single In(Ga)As/InAs QD using a wide range of laser tuning relative to the exciton transition in the QD, enabling us to quantify the level of robustness of this control scheme in the context of practical QD systems possessing variations in QD size. Our findings indicate that, in contrast to Rabi rotations for which the detuning dependence of the maximum exciton occupation follows the spectrum of the laser pulse and is highly sensitive to pulse area, the use of frequency-swept pulses in ARP enables a dramatic increase in the tolerance to differences in the optical properties of the QDs. We demonstrate a high exciton inversion efficiency over a 20 meV laser tuning bandwidth using broadband control pulses with a pulse area of 2.5π, spectral chirp of 100,000 fs^2, and control pulse duration of 2.3 ps. Since this detuning bandwidth is comparable to typical variations in both the GS optical transition energies and the energy separation between the GS and ES transitions in self-assembled QD ensembles, our results indicate that ARP is an ideal control scheme for realizing parallel quantum state initialization of multiple QD quantum emitters. Our numerical simulations provide excellent agreement with our experimental results and indicate that the use of a positive pulse chirp for ARP is essential to maximize the detuning bandwidth at low pulse areas. Our findings will support the development of quantum networks and linear optical computing platforms utilizing semiconductor QDs.

Funding. Natural Sciences and Engineering Research Council of Canada (RGPIN-2020-06322).

Disclosures. The authors declare no conflicts of interest.

Data availability. Data underlying the results presented in this paper are not publicly available at this time but may be obtained from the authors upon reasonable request.

Supplemental document. See Supplement 1 for supporting content.

References

1. E. Knill, R. Laflamme, and G. J. Milburn, "A scheme for efficient quantum computation with linear optics," Nature **409**(6816), 46–52 (2001).
2. M. Atature, D. Englund, N. Vamivakas, S.-Y. Lee, and J. Wrachtrup, "Material platforms for spin-based photonic quantum technologies," Nat. Rev. Mater. **3**(5), 38–51 (2018).
3. P. G. Eliseev, H. Li, A. Stintz, G. T. Liu, T. C. Newell, K. J. Malloy, and L. F. Lester, "Transition dipole moment of InAs/InGaAs quantum dots from experiments on ultralow-threshold laser diodes," Appl. Phys. Lett. **77**(2), 262–264 (2000).
4. T. H. Stievator, X. Li, D. G. Steel, D. Gammon, D. S. Katzer, D. Park, C. Piermarocchi, and L. J. Sham, "Rabi oscillations of excitons in single quantum dots," Phys. Rev. Lett. **87**(13), 133603 (2001).
5. H. Kamada, H. Gotoh, J. Temmyo, T. Takagahara, and H. Ando, "Exciton Rabi oscillation in a single quantum dot," Phys. Rev. Lett. **87**(24), 246401 (2001).
6. D. Dalacu, P. J. Poole, and R. L. Williams, "Nanowire-based sources of non-classical light," Nanotechnology **30**(23), 232001 (2019).

Optics EXPRESS

7. P. Senellart, G. Solomon, and A. White, "High-performance semiconductor quantum-dot single photon sources," Nat. Nanotechnol. **12**(11), 1026–1039 (2017).
8. D. Huber, M. Reindl, J. Aberl, A. Rastelli, and R. Trotta, "Semiconductor quantum dots as an ideal source of polarization-entangled photon pairs on-demand: a review," J. Opt. **20**(7), 073002 (2018).
9. P. Michler, A. Kiraz, C. Becher, W. V. Schoenfeld, P. M. Petroff, L. Zhang, E. Hu, and A. Imamoglu, "A quantum dot single-photon turnstile device," Science **290**(5500), 2282–2285 (2000).
10. C. Santori, D. Fattal, J. Vuckovic, G. S. Solomon, and Y. Yamamoto, "Indistinguishable photons from a single-photon device," Nature **419**(6907), 594–597 (2002).
11. S. Ates, S. M. Ulrich, S. Reitzenstein, A. Loffler, A. Forchel, and P. Michler, "Post-selected indistinguishable photons from the resonance fluorescence of a single quantum dot in a microcavity," Phys. Rev. Lett. **103**(16), 167402 (2009).
12. O. Gazzano, S. Michaelis de Vasconcellos, C. Arnold, A. Nowak, E. Galopin, I. Sagnes, L. Lanco, A. Lemaitre, and P. Senellart, "Bright solid-state sources of indistinguishable single photons," Nat. Commun. **4**(1), 1425 (2013).
13. V. Giesz, S. L. Portalupi, T. Grange, C. Anton, L. De Santis, J. Demory, N. Somaschi, I. Sagnes, A. Lemaitre, L. Lanco, A. Auffeves, and P. Senellart, "Cavity-enhanced two-photon interference using remote quantum dot sources," Phys. Rev. B **92**(16), 161302 (2015).
14. N. Somaschi, V. Giesz, L. De Santis, J. C. Loredo, M. P. Almeida, G. Hornecker, S. L. Portalupi, T. Grange, C. Anton, J. Demory, C. Gomez, I. Sagnes, N. D. Lanzillotti-Kimura, A. Lemaitre, A. Auffeves, A. G. White, L. Lanco, and P. Senellart, "Near-optimal single-photon sources in the solid state," Nat. Photonics **10**(5), 340–345 (2016).
15. M. Reindl, K. D. Jons, D. Huber, C. Schimpf, Y. Huo, V. Zwiller, A. Rastelli, and R. Trotta, "Phonon-assisted two-photon interference from remote quantum emitters," Nano Lett. **17**(7), 4090–4095 (2017).
16. C. Gustin and S. Hughes, "Influence of electron-phonon scattering for an on-demand quantum dot single-photon source using cavity-assisted adiabatic passage," Phys. Rev. B **96**(8), 085305 (2017).
17. P. Gold, A. Thoma, S. Maier, S. Reitzenstein, C. Schneider, S. Hofling, and M Kamp, "Two-photon interference from remote quantum dots with inhomogeneously broadened linewidths," Phys. Rev. B **89**(3), 035313 (2014).
18. A. Thoma, P. Schnauber, J. Bohm, M. Gschrey, J.-H. Schulze, A. Strittmatter, S. Rodt, T. Heindel, and S. Reitzenstein, "Two-photon interference from remote deterministic quantum dot micolenses," Appl. Phys. Lett. **110**(1), 011104 (2017).
19. N. Akopian, N. H. Lindner, E. Poem, Y. Berlatzky, J. Avron, D. Gershoni, B. D. Geradot, and P. M. Petroff, "Entangled photon pairs from semiconductor quantum dots," Phys. Rev. Lett. **96**(13), 130501 (2006).
20. T. Heindel, A. Thoma, M. von Helversen, M. Schmidt, A. Schlehahn, M. Gschrey, P. Schnauber, J.-H. Schulze, A. Strittmatter, J. Beyer, S. Rodt, A. Carmele, A. Knorr, and S. Reitzenstein, "A bright triggered twin-photon source in the solid state," Nat. Commun. **8**(1), 14870 (2017).
21. S. Bounouar, M. Straub, A Carmele, P. Schnauber, A. Thoma, M. Gschrey, J.-H. Schulze, A. Strittmatter, S. Rodt, A. Knorr, and S. Reitzenstein, "Path-controlled time reordering of paired photons in a dressed three-level cascade," Phys. Rev. Lett. **118**(23), 233601 (2017).
22. R. Winik, D. Cogan, Y. Don, I. Schwartz, L. Gantz, E. R. Schmidgall, N. Livneh, R. Rapaport, E. Buks, and D. Gershoni, "On-demand source of maximally entangled photon pairs using the biexciton-exciton radiative cascade," Phys. Rev. B **95**(23), 235435 (2017).
23. Y. Chen, M. Zopf, R. Keil, F. Ding, and O. G. Schmidt, "Highly-efficient extraction of entangled photons from quantum dots using a broadband optical antenna," Nat. Commun. **9**(1), 2994 (2018).
24. R. Trotta, J. Martin-Sanchez, J. S. Wildmann, G. Piredda, M. Reindl, C. Schimpf, E. Zallo, S. Stroj, J. Edlinger, and A. Rastelli, "Wavelength-tunable sources of entangled photons interfaced with atomic vapours," Nat. Commun. **7**(1), 10375 (2016).
25. E. B. Flagg, A. Muller, S. V. Polyakov, A. Ling, A. Migdall, and G. S. Solomon, "Interference of single photons from two separate semiconductor quantum dots," Phys. Rev. Lett. **104**(13), 137401 (2010).
26. R. B. Patel, A. J. Bennett, K. Cooper, P. Atkinson, C. A. Nicoll, D. A. Ritchie, and A. J. Shields, "Quantum interference of electrically generated single photons from a quantum dot," Nanotechnology **21**(27), 274011 (2010).
27. A. Zrenner, E. Beham, S. Stufler, F. Findeis, M. Bichler, and G. Abstreiter, "Coherent properties of a two-level system based on a quantum-dot photodiode," Nature **418**(6898), 612–614 (2002).
28. H. Htoon, T. Takagahara, D. Kulik, O. Baklenov, A. L. Holmes Jr., and C. K. Shih, "Interplay of Rabi oscillations and quantum interference in semiconductor quantum dots," Phys. Rev. Lett. **88**(8), 087401 (2002).
29. S. Stufler, P. Machnikowski, P. Ester, M. Bichler, V. M. Axt, T. Kuhn, and A. Zrenner, "Two-photon Rabi oscillations in a single $In_xGa_1 - xAs/GaAs$ quantum dot," Phys. Rev. B **73**(12), 125304 (2006).
30. H. Jayakumar, A. Predojevic, T. Huber, T. Kauten, G. S. Solomon, and G. Weihs, "Deterministic photon pairs and coherent optical control of a single quantum dot," Phys. Rev. Lett. **110**(13), 135505 (2013).
31. M. M. T. Loy, "Observation of population inversion by optical adiabatic rapid passage," Phys. Rev. Lett. **32**(15), 814–817 (1974).
32. V. S. Malinovsky and J. L. Krause, "General theory of population transfer by adiabatic rapid passage with intense, chirped laser pulses," Eur. Phys. J. D **14**(2), 147–155 (2001).
33. B. W. Shore, *Manipulating quantum structures using laser pulses*, (Cambridge University, 2011), pp 513–521.
34. C.-M. Simon, T. Belhadj, B. Chatel, T. Amand, P. Renucci, A. Lemaitre, O. Krebs, P. A. Dalgarno, R. J. Warburton, X. Marie, and B. Urbaszek, "Robust quantum dot exciton generation via adiabatic rapid passage with frequency-swept optical pulses," Phys. Rev. Lett. **106**(16), 166801 (2011).

Optics EXPRESS

35. Y. Wu, I. M. Piper, M. Ediger, P. Brereton, E. R. Schmidgall, P. R. Eastham, M. Hugues, M. Hopkinson, and R. T. Phillips, "Population inversion in a single InGaAs quantum dot using the method of adiabatic rapid passage," Phys. Rev. Lett. **106**(6), 067401 (2011).
36. R. Mathew, E. Dilcher, A. Gamouras, A. Ramachandran, H. Y. S. Yang, S. Freisem, D. Deppe, and K. C. Hall, "Subpicosecond adiabatic rapid passage on a single semiconductor quantum dot: Phonon-mediated dephasing in the strong-driving regime," Phys. Rev. B **90**(3), 035316 (2014).
37. A. Gamouras, R. Mathew, S. Freisem, D. G. Deppe, and K. C. Hall, "Simultaneous deterministic control of distant qubits in two semiconductor quantum dots," Nano Lett. **13**(10), 4666–4670 (2013).
38. T. Kaldewey, S. Luker, A. V. Kuhlmann, S. R. Valentin, A. Ludwig, A. D. Wieck, D. E. Reiter, T. Kuhn, and R. J. Warburton, "Coherent and robust high-fidelity generation of a biexciton in a quantum dot by rapid adiabatic passage," Phys. Rev. B **95**(16), 161302 (2017).
39. Y.-J. Wei, Y.-M. He, M.-C. Chen, Y.-N. Hu, Y. He, D. Wu, C. Schneider, M. Kamp, S. Hofling, C.-Y. Lu, and J.-W. Pan, "Deterministic and robust generation of single photons from a single quantum dot with 99.5% indistinguishability using adiabatic rapid passage," Nano Lett. **14**(11), 6515–6519 (2014).
40. T. Kaldewey, S. Luker, A. V. Kuhlmann, S. R. Valentin, J.-M. Chauveau, A. Ludwig, A. D. Wieck, D. E. Reiter, T. Kuhn, and R. J. Warburton, "Demonstrating the decoupling regime of the electron-phonon interaction in a quantum dot using chirped pulse optical excitation," Phys. Rev. B **95**(24), 241306 (2017).
41. A. Ramachandran, G. R. Wilbur, S. O.'Neal, D. G. Deppe, and K. C. Hall, "Suppression of decoherence tied to electron-phonon coupling in telecom-compatible quantum dots: low-threshold reappearance regime for quantum state inversion," Opt. Lett. **45**(23), 6498–6501 (2020).
42. T. F. Boggess, L. Zhang, D. G. Deppe, D. L. Huffaker, and C. Cao, "Spectral engineering of carrier dynamics in In(Ga)As self-assembled quantum dots," Appl. Phys. Lett. **78**(3), 276–278 (2001).
43. J. L. Robb, Y. Chen, A. Timmons, K. C. Hall, O. B. Shchekin, and D. G. Deppe, "Time-resolved Faraday rotation measurements of spin relaxation in InGaAs/GaAs quantum dots: Role of excess energy," Appl. Phys. Lett. **90**(15), 153118 (2007).
44. A. Mohan, P. Gallo, M. Felici, B. Dwir, A. Rudra, J. Faist, and E. Kapon, "Record-low inhomogeneous broadening of site-controlled quantum dots for nanophotonics," Small **6**(12), 1268–1272 (2010).
45. P.-L. Ardelt, L. Hanschke, K. A. Fischer, K. Muller, A. Kleinkauf, M. Koller, A. Bechtold, T. Simmet, J. Wierzbowski, H. Riedl, G. Abstreiter, and J. L. Finley, "Dissipative preparation of the exciton and biexciton in self-assembled quantum dots on picosecond time scales," Phys. Rev. B **90**(24), 241404 (2014).
46. J. H. Quilter, A. J. Brash, F. Liu, M. Glassl, A. M. Barth, V. M. Axt, A. J. Ramsay, M. S. Skolnick, and A. M. Fox, "Phonon-assisted population inversion of a single InGaAs/GaAs quantum dot by pulsed laser excitation," Phys. Rev. Lett. **114**(13), 137401 (2015).
47. A. J. Ramsay, "A review of the coherent optical control of the exciton and spin states of semiconductor quantum dots," Semicond. Sci. Technol. **25**(10), 103001 (2010).
48. S. Luker and D. E. Reiter, "A review on optical excitation of semiconductor quantum dots under the influence of phonons," Semicond. Sci. Technol. **34**(6), 063002 (2019).
49. V. V. Lozovoy, I. Pastirk, and M. Dantus, "Multiphoton intrapulse interference. IV. Ultrashort laser pulse spectral phase characterization and compensation," Opt. Lett. **29**(7), 775–777 (2004).
50. A. Gamouras, R. Mathew, and K. C. Hall, "Optically engineered ultrafast pulses for controlled rotations of exciton qubits in semiconductor quantum dots," J. Appl. Phys. **112**(1), 014313 (2012).
51. J. Forstner, C. Weber, J. Danckwerts, and A. Knorr, "Phonon-assisted damping of Rabi oscillations in semiconductor quantum dots," Phys. Rev. Lett. **91**(12), 127401 (2003).
52. A. Krugel, V. M. Axt, T. Kuhn, P. Machnikowski, and A. Vagov, "The role of acoustic phonons for Rabi oscillations in semiconductor quantum dots," Appl. Phys. B **81**(7), 897–904 (2005).
53. A. J. Ramsay, A. V. Gopal, E. M. Gauger, A. Nazir, B. W. Lovett, A. M. Fox, and M. S. Skolnick, "Damping of exciton Rabi rotations by acoustic phonons in optically excited InGaAs/GaAs quantum dots," Phys. Rev. Lett. **104**(1), 017402 (2010).
54. A. Debnath, C. Meier, B. Chatel, and T. Amand, "Chirped laser excitation of quantum dot excitons coupled to a phonon bath," Phys. Rev. B **86**(16), 161304 (2012).
55. A. Debnath, C. Meier, B. Chatel, and T. Amand, "High-fidelity biexciton generation in quantum dots by chirped laser pulses," Phys. Rev. B **88**(20), 201305 (2013).
56. R. Mathew, C. E. Pryor, M. E. Flatte, and K. C. Hall, "Optimal quantum control for conditional rotation of exciton qubits in semiconductor quantum dots," Phys. Rev. B **84**(20), 205322 (2011).
57. A. J. Ramsay, T. M. Godden, S. J. Boyle, E. M. Gauger, A. Nazir, B. W. Lovett, A. V. Gopal, A. M. Fox, and M. S. Skolnick, "Effect of detuning on the phonon induced dephasing of optically-driven InGaAs/GaAs quantum dots," J. Appl. Phys. **109**(10), 102415 (2011).
58. A. Gamouras, M. Britton, M. M. Khairy, R. Mathew, D. Dalacu, P. Poole, D. Poitras, R. L. Williams, and K. C. Hall, "Energy-selective optical excitation and detection in InAs/InP quantum dot ensembles using a one-dimensional optical microcavity," Appl. Phys. Lett. **103**(25), 253109 (2013).
59. H. Htoon, D. Kulik, O. Baklenov, A. L. Holmes T. Takagahara, and C. K. Shih, "Carrier relaxation and quantum decoherence of excited states in self-assembled quantum dots," Phys. Rev. B **63**(24), 241303 (2001).